Tip-Induced Reduction of the Resonant Tunneling Current on Semiconductor Surfaces

Pavel Jelínek,[1,*] Martin Švec,[1] Pablo Pou,[2] Ruben Perez,[2] and Vladimír Chráb[1]

[1]*Institute of Physics, Academy of Sciences of the Czech Republic, Cukrovarnicka 10, 1862 53, Prague, Czech Republic*
[2]*Departamento de Física Teórica de la Materia Condensada, Universidad Autónoma de Madrid, E-28049 Madrid, Spain*

(Received 23 July 2008; published 21 October 2008)

We report scanning tunneling microscope measurements showing a substantial decrease of the current, almost to zero, on the Si(111)-(7×7) reconstruction in the near-to-contact region under low bias conditions. First principles simulations for the tip-sample interaction and transport calculations show that this effect is driven by the substantial local modification of the atomic and electronic structure of the surface. The chemical reactivity of the adatom dangling bond states that dominate the electronic density of states close to the Fermi level and their spatial localization result in a strong modification of the electronic current.

DOI: 10.1103/PhysRevLett.101.176101 PACS numbers: 68.37.Ef, 73.20.−r, 73.63.Rt

The development of local probe techniques such as the scanning tunneling microscope (STM) [1] and atomic force microscopy (AFM) [2] has allowed real-space imaging and modification of surfaces at the atomic scale [3]. While standard STM imaging is done mostly in the tunneling regime, many recent applications, including atomic and molecular manipulation [4–6], take place in the near-to-contact regime. In this distance range, the tip-sample interaction is expected to modify the structural and electronic properties of the surface, making the quantitative interpretation of the experimental transport measurements far more difficult. Recent advances in the experimental setup for dynamic AFM [7] allow the simultaneous acquisition of both the tunneling current and the atomic forces [6,8], paving the way for a precise characterization of the evolution of these quantities up to the contact formation.

In the elementary quantum mechanics courses we learn that the tunneling current grows exponentially with a decrease of the width of the tunneling barrier or, in the context of STM measurements, with a reduction of the tip-sample distance. However, this basic assumption has to be carefully reexamined at distances where the onset of the short-range chemical interaction between the probe apex and the surface adatoms occurs [9,10]. Deviations from the exponential behavior of the tunneling current were already reported by Clarke *et al.* [11] on metal surfaces and attributed to the relaxations induced by the tip-sample interaction. The role of these forces in the large vertical corrugations found experimentally on close-packed metallic surfaces has been extensively investigated both experimental and theoretically [9,10,12].

These studies reveal that the interaction regime along the tip-sample distance can be divided into three parts: (i) the tunneling regime, (ii) the near-to-contact regime, and (iii) the contact regime. At the tunneling regime, corresponding to large tip-sample distances, the surface structure remains practically unchanged and the current shows an exponential decay along the distance. Approaching the near-to-contact regime, the proximity of a probe induces a rapid increase of the short-range chemical interaction between the tip apex atom and the surface atom, that is accompanied by a strong vertical relaxation of the surface atom [13]. Therefore, a significant modification of both the atomic and electronic structure [14,15] of the surface is expected. In this regime, the increase of the current is still observed on metallic systems. Nevertheless, the exponential relation is no longer valid due to the presence of the large atomic relaxations and the relevance of electron multiple-scattering events in the tunneling process [9]. To properly address this regime, it is necessary to adopt theoretical techniques going beyond a simple perturbative scheme for the tunneling current [9,16]. Further approach of the probe leads to a collapse of the tunneling barrier (as seen also in semiconductor surfaces [17]). The atomic contact is then fully established and electrons propagate in ballistic regime between tip and sample [18]. The contact formation between a metallic tip and molecular species adsorbed on metal [19] and semiconductor surfaces [20] has been recently explored. These studies confirm a rapid increase in the conductance in the transition from the tunneling to the contact regime.

In this work, we show that the commonly accepted picture discussed above fails to describe the electronic transport on semiconductor surfaces under low bias conditions, where electron transfer is mainly driven by a resonant tunneling process through strongly localized dangling bond states. Here, we report a substantial decrease of the current, almost to zero, on a semiconductor surface at an intermediate tip-sample distance. We combine these STM measurements on the Si(111)-(7×7) with first principles simulations based on density functional theory (DFT) and transport calculations to show that this effect is driven by the substantial local modification of the atomic and electronic structure of the surface induced by the short-range chemical interaction between the tip apex atom and the surface adatom. The chemical reactivity of the adatom dangling bond states, that dominate the electronic density of states close to the Fermi level, and their spatial local-

ization result in a strong modification of the electronic current. Consequently, in the STM images measured at these tip-sample distances, the current drop can induce the inversion of the atomic STM contrast observed at the tunneling regime (see [21]).

STM measurements were performed with a standard Omicron VT STM instrument at room temperature (RT). The sample was a $10 \times 2 \times 0.5$ mm^3 strip cut from a common p-type Si wafer with a bulk conductivity of 1–10 $\Omega \cdot \mathrm{cm}^{-1}$. The surface was prepared *in situ* by repeated flashing up to 1150 °C followed by slow cooling to RT. The pressure in the UHV chamber did not exceed 5×10^{-10} mbar during this procedure. Annealing was achieved by passing a direct current through the sample. The tip used in the experiments was etched of a ø 0.2 mm *W* wire and annealed in UHV by heat emission from a hot *W* filament. The STM microscope was operated in the constant-height mode using weak feedback [22] and a low bias voltage below 0.2 V at both polarities. To minimize a lateral movement of the tip during the measurement of the I-z curves, only a small area was explored and the thermal drift was settled below a speed of 0.1 Å/s. For the I-z measurement, the scanning was stopped above the Si adatoms, the feedback loop was switched off and the current was measured as a function of the varying tip-sample distance with a total of 100 points within 1 s. The extent of the tip movement towards the sample was typically 4.0 Å. Measurements were performed at both polarities of the bias voltage and for both directions of the tip movement. Under these conditions, the I-z curves were perfectly reproducible over equivalent adatoms in the 7×7 unit cell. A constant-height image of the area was acquired after the I-z measurement to exclude any surface alteration. The conductance was calculated using the expression $G = I/V$, with I the current and V the sample voltage.

In the Si(111)-(7×7) reconstruction, the partially filled adatom dangling bond states localized near the Fermi level determine the metallic character of the surface [23]. Consequently, the STM current between tip and sample at low bias voltage flows entirely through these adatom dangling bonds in both polarities. A typical constant-height image (left inset of Fig. 1), taken at bias voltage of -0.2 V (tunneling to the sample filled states), shows adatoms as bright protrusions.

Figure 1 represents a characteristic set of G-z curves recorded during one STM session at a bias voltage of -0.2 V over randomly selected adatoms of the 7×7 unit cell. At large tip-sample distances, the conductance increases almost exponentially with the decrease of the tip-sample distance (see the linear behavior of G vs d plotted in a logarithmic scale in the inset of Fig. 1). However, around a tip-sample distance of -1.6 Å a slight deviation from the exponential dependence is observed. Approaching the tip further towards the surface, just after the conductance reaches a peak of $\sim 0.002\ G_0$, a sudden drop of

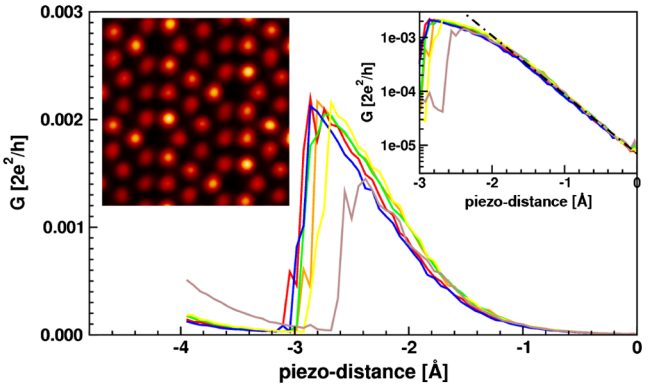

FIG. 1 (color online). Experimental G-z curves acquired at $V = -200$ mV over different adatoms within 7×7 unit cell. The origin of the tip-sample distance has been assigned to the offset current value $I_0 = 0.12$ nA. The left inset shows a typical current image of the explored area (5 nm × 5 nm). The right inset plots the G-z curves in logarithmic scale to demonstrate the exponential decay of the conductance with the increasing tip-sample distance.

the conductance almost to zero is observed (see also [21]). Further decrease of the tip-sample distance leads again to the conductance increase. After that, the tip was retracted to its initial vertical position and a lateral current scan at large tip-sample distance was performed to confirm that the surface was not modified. The details of the G-z curves, the slope $d \ln I/dz$ and the conductance maxima, vary due to the modification of the atomic structure of the probe. For example, the conductance peak can change from 0.002 to 0.008 G_0. However, the overall structure of the curve and, in particular, the conductance drop, have been well reproduced during various experimental sessions, independently of a vertical movement of the tip to or from the surface and in both polarities (see [21]). On the other hand, at bias voltages larger than -0.5 V, we were unable to detect the conductance drop in our measurements and we recover the behavior reported previously [17].

From performed DFT calculations, we have been able to follow the atomic relaxations of both tip and sample atoms, the accompanying changes in the electronic DOS and the influence of these two factors in the electron transport at different tip-sample distances.

Our theoretical study of the Si(111)-(7×7) surface in the presence of an STM tip has been performed with the FIREBALL DFT code [24]. A slab approach, including 7 Si layers and an additional H-passivating layer, has been used to model the surface [5]. As the probe model, we have adopted a pyramid of ten tungsten atoms with (100) surface orientation. The whole system contains in total 347 atoms. We have subsequently approached the tip in a quasistatic manner at zero temperature, at each step leaving the first six top Si layers of the slab and the five outermost tungsten tip atoms to relax according to their optimal position. The rest of the atoms were kept fixed in their bulklike configuration. The atomic positions were converged until

the following energy and force criteria, 10^{-6} eV and 0.05 eV/Å, respectively, were satisfied. Calculations of the STM current were carried out using a Green's function formalism [9]. Both the total energy and the STM current calculations were performed sampling only the Γ k point of the surface Brillouin zone.

Our theoretical results (see Fig. 2) reproduce the exponential behavior at large distances and the sudden drop of the conductance (at a distance of 4.75 Å with a conductance maxima of 0.015 G_0). Figures 2(a) and 2(b) unveil a strong correlation between the upward adatom displacement, the decrease of the conductance and the formation of the chemical bond between the apex atom and the surface adatom. At large tip-sample distances, there is no significant vertical displacement of the adatom [see Fig. 2(b)]. A large upward movement of the adatom, around 0.5 Å, is observed around the tip-sample distances of ~5 Å. At the same distance, a rapid variation of the short-range chemical force between tip and sample takes place [see Fig. 2(a)]. Next, the vertical adatom displacement decreases until it reaches its initial value at a tip-sample distance near to 3 Å.

A detailed analysis of the electronic structure of the adatom along the tip-sample distance, see Fig. 2(c), sheds light on the origin of the unusual drop of the STM conductance. In the tunneling regime, the dangling bond state remains in a similar energy as on the unperturbed surface. Reaching tip-sample distances ~5 Å, where the formation of the chemical bond between tip and sample takes place, we observe a strong modification of the local electronic state of the inspected surface adatom. At closer tip-sample distances, below 5 Å, the dangling bond state is completely wiped off from the Fermi level, as it can be seen

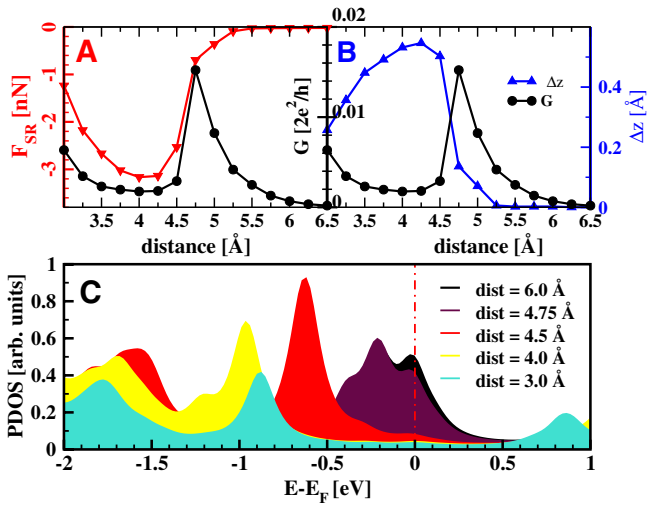

FIG. 2 (color online). (a) Evolution of the quantum conductance G (right axis) and the atomic force (left axis) as a function of the tip-sample distance, (b) the quantum conductance (left axis) and the vertical adatom displacement (right axis) as a function of the tip-sample distance, (c) PDOS of silicon corner adatom as a function of the tip-sample distance.

on Fig. 2(c). This rigid displacement of the center of the valence band, ~0.8 eV below the Fermi level, together with the strong spatial localization of the dangling bond orbitals—that limits the tunneling through the surrounding adatoms—explains naturally the drastic decrease of the conductance at low bias voltages. This conductance drop is not found at higher bias voltages, where the position of the valence band lies within the energy range where the transfer electron comes [21]. The increase of the conductance observed with the further reduction of the tip-sample distance after the conductance drop is mainly driven by the electron transfer between the tip and surrounding surface atoms.

In order to analyze the redistribution of electronic charges on the surface due to the proximity of the probe, we have calculated the real-space electron density near the Fermi level. Electron charge isosurfaces at 0.005 $e/\text{Å}^3$ in the energy range between the Fermi level and -0.4 eV for different tip-sample distances are shown in Fig. 3. The first snapshot shows the characteristic distribution of the clean Si(111)-(7 × 7) surface, where dangling bond states are well localized on individual adatoms. The next snapshot, corresponding to the tip-sample distance 4.75 Å, just before the conductance drop, reveals a charge transfer from the adatom to its neighbors, which leads to charge accumulation on the closer rest atoms. In the third image, taken at the distance 4.5 Å, the electron charge corresponding to the adatom dangling bond is no longer present in the relevant energy window, preventing the electron transport between the tip and the surface through this dangling bond. The electron charge accumulated on the rest atoms is still well visible but it decreases with further approach of the tip towards the surface. On the other hand, the distribution of the tip charge densities remains practically unchanged during the whole approach path. This fact confirms the idea that the conductance drop is mainly related to the local change of the electronic structure of the surface.

From the scenario described above, it is evident that electron transport on semiconductor surfaces with strongly localized surface states is different from metallic surfaces, where the transport mainly occurs through delocalized *sp-like* states, which are, in principle, less sensitive to the additional hybridization due to the presence of a tip. However, the situation can change in the case of more localized *d-like* states. Recently, Néel *et al.* [14] showed how a shift of a *d* state of Co atoms on a Cu(100) surface induced by the tip proximity affects the Kondo temperature. It is worth mentioning that similar G-z curves have been also observed on the center Si adatoms within the Si(111)-(7 × 7) unit cell in both experiments and theoretical simulations. The modification of the DOS induced by the tip proximity may provide an explanation for the interplay between forces and bias voltage found in recent experiments [15]. Furthermore, we have also found, based on our first principles DFT simulations, a similar behavior on the α-Sn/Si(111)-($\sqrt{3} \times \sqrt{3}$) surface. Thus, we expect this

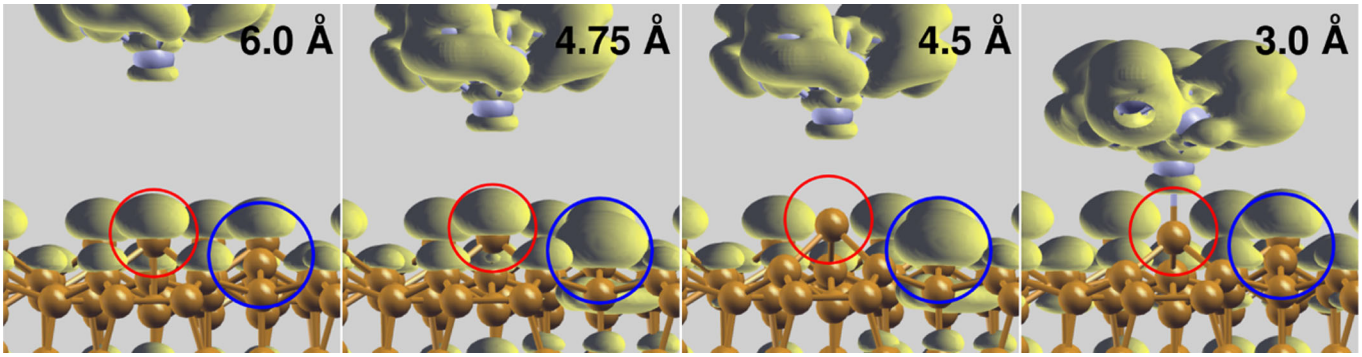

FIG. 3 (color online). Isosurfaces of electron charge density 0.005 $e/\text{Å}^3$ integrated in the E_F-E_F − 0.4 eV range, for different tip-sample distances. The probe is placed over the corner adatom in the Si(111)-(7 × 7) faulted unit cell. The Si adatom is marked by a red cycle and the Si rest atom by a blue cycle.

phenomena to be found not only in semiconductor surfaces, but in many other systems, e.g., atoms and molecules on surfaces, where the electron transport occurs through strongly localized states near the Fermi level.

In conclusion, we have reported a nontrivial behavior of the STM current along the tip-sample distance on semiconductor surfaces. To summarize, we have observed a substantial decrease of the STM conductance during the approach of the tip to the semiconductor surface and we have confirmed it with first-principle DFT calculations. The detailed analysis of the local density of states of the inspected Si adatom unveils the origin of the conductance drop at closer tip-sample distances. We attribute this unusual feature of the conductance to the formation of the strong covalent bond between the tip apex atom and the adatom which induces the vertical displacement and the LDOS changes of the adatom.

This work was supported from Grants No. IAA1010413, AV0Z10100521, KAN400100701 and IAA100100616. The work of P. P. and R. P. is supported by the Project MAT2005-01298 (MICINN, Spain).

*Corresponding author.
jelinekp@fzu.cz

[1] G. Binnig, H. Rohrer, Ch. Gerber, and E. Weibel, Phys. Rev. Lett. **49**, 57 (1982).
[2] G. Binnig, C. F. Quate, and Ch. Gerber, Phys. Rev. Lett. **56**, 930 (1986).
[3] F. J. Giessibl, Rev. Mod. Phys. **75**, 949 (2003).
[4] Y. Sugimoto, P. Pou, M. Abe, P. Jelinek, R. Pérez, S. Morita, and O. Custance, Nature (London) **446**, 64 (2007).
[5] Y. Sugimoto, P. Jelinek, P. Pou, M. Abe, S. Morita, R. Pérez, and O. Custance, Phys. Rev. Lett. **98**, 106104 (2007).
[6] M. Ternes, Ch. P. Lutz, C. F. Hirjibehedin, F. J. Giessibl, and A. J. Heinrich, Science **319**, 1066 (2008).
[7] F. J. Giessibl, Appl. Phys. Lett. **73**, 3956 (1998).
[8] S. Hembacher, F. J. Giessibl, J. Mannhart, and C. F. Quate, Phys. Rev. Lett. **94**, 056101 (2005).
[9] J. M. Blanco, C. Gonzalez, P. Jelínek, J. Ortega, F. Flores, and R. Pérez, Phys. Rev. B **70**, 085405 (2004).
[10] W. A. Hofer, A. J. Fisher, R. A. Wolkow, and P. Grutter, Phys. Rev. Lett. **87**, 236104 (2001).
[11] A. R. H. Clarke, J. B. Pethica, J. A. Nieminen, F. Besenbacher, E. Lægsgaard, and I. Stensgaard, Phys. Rev. Lett. **76**, 1276 (1996).
[12] A. Schirmeisen, G. Cross, A. Stalder, P Grutter, and U. Durig, New J. Phys. **2**, 29 (2000).
[13] Y. Sugimoto, O. Custance, S. Morita, M. Abe, P. Pou, P. Jelínek, and R. Pérez, Phys. Rev. B **73**, 205329 (2006).
[14] N. Néel, J. Kroger, L. Limot, K. Palotas, W. A. Hofer, and R. Berndt, Phys. Rev. Lett. **98**, 016801 (2007).
[15] T. Arai and M. Tomitori, Phys. Rev. Lett. **93**, 256101 (2004).
[16] K. H. Bevan, F. Zahid, D. Kienle, and H. Guo, Phys. Rev. B **76**, 045325 (2007).
[17] C. J. Chen and R. J. Hamers, J. Vac. Sci. Technol. B **9**, 503 (1991).
[18] N. Agrait, A. Levy-Yeyati, and J. van Ruitenbeek, Phys. Rep. **377**, 81 (2003).
[19] N. Néel, J. Kroger, L. Limot, T. Frederiksen, M. Brandbyge, and R. Berndt, Phys. Rev. Lett. **98**, 065502 (2007).
[20] B. Naydenov, L. C. Teague, P. Ryan, and J. J. Boland, Nano Lett. **6**, 1752 (2006).
[21] See EPAPS Document No. E-PRLTAO-101-009843 for additional figures. For more information on EPAPS, see http://www.aip.org/pubservs/epaps.html.
[22] M. Švec, P. Jelínek, P. Shukrynau, C. González, V. Cháb, and V. Drchal, Phys. Rev. B **77**, 125104 (2008).
[23] K. Takayanagi, Y. Tanishiro, M. Takahashi, and S. Takahashi, Surf. Sci. **164**, 367 (1985).
[24] P. Jelinek, H. Wang, J. P. Lewis, O. F. Sankey, and J. Ortega, Phys. Rev. B **71**, 235101 (2005).